MIMO Receiver with Reduced Number of RF Chains Based on 4D Array and Software Defined Radio

Grzegorz Bogdan
Warsaw University of Technology
Warsaw, Poland
g.bogdan@ire.pw.edu.pl

Konrad Godziszewski
Warsaw University of Technology
Warsaw, Poland
k.godziszewski@ire.pw.edu.pl

Yevhen Yashchyshyn
Warsaw University of Technology
Warsaw, Poland
y.yashchyshyn@ire.pw.edu.pl

***Abstract*—Multiple-input multiple-output (MIMO) technique is expected to be extensively used in future wireless systems to increase capacity of wireless channels. Nevertheless, the capacity gain comes with a cost. In particular, multiple analog radio frequency (RF) chains are required at both the transmitter and the receiver, thereby leading to a higher implementation cost, more power consumption, and lower energy efficiency. This paper presents a receiver with only one RF chain for 2×2 MIMO transmission system. Proposed design is based on a time modulated antenna array (TMAA) with beam-steering functionality and a wideband software defined radio (SDR). Spatial streams were created by demultiplexing spectral components (sidebands) generated by periodical ON/OFF switching. Number of RF chains was reduced from 2 to 1 while maintaining sufficiently low correlation of spatial streams, which is required to perform MIMO transmission. Feasibility of proposed technique is evaluated by means of experimental verification.**

***Index Terms*—antenna array, adaptive antenna, 4D array, time modulated antenna array, beam-steering, multiple-input multiple-output**

I. Introduction

Multiple-input multiple-output (MIMO) techniques are extensively used to increase capacity of the wireless channel by exploiting the spatial properties of the multipath environments [1]. Unfortunately, the high cost and power consumption of components like analog-to-digital converters constrains feasibility of MIMO in low–cost wireless devices. The issue of reducing the number of radio frequency (RF) chains in MIMO systems while retaining their performance was addressed in many research papers. Two main approaches are antenna selection [2] and hybrid (analog and digital) combining/precoding [3], [4]. These schemes can provide performance close to that of a system utilizing a dedicated RF chain for each receive antenna with less number of RF chains and without increasing the overall complexity.

Another issue of MIMO systems is the assumption of statistically independent spatial streams which is satisfied to some degree in environments with multipath propagation. Recent research proved that correlation of spatial streams can be decreased by taking advantage of the key parameters of antennas [5]. For instance, diversity can be produced with distinct radiation patterns, i.e. highly orthogonal patterns create low correlation, hence capacity gains are possible. A rather interesting topic for active research is to find out newer antenna design which can produce high orthogonality between the radiation patterns [6].

Time modulated antenna array (TMAA, also referred to as four-dimentional or 4D array) uses time as an additional degree of freedom in antenna beamforming [7]. Operational principles is based on fast switching which generates spectral components (sidebands) located at multiples of the modulation frequency around the center frequency. Suitability of sidebands for hybrid precoding for MIMO systems was thoroughly studied in [8]. In [9] utilization of sidebands as virtual MIMO streams was investigated experimentally with a setup composed of two transmitting software defined radios (SDRs) and only one receiving SDR with TMAA.

In this paper we demonstrate a MIMO received based on SDR and 4D array with improved performance, i.e. the receiving RF chain has wider bandwidth (160 MHz) and the TMAA supports reception of wideband signals.

II. 4D array fundamentals

Typically, TMAA utilizes single–pole single–throw (SPST) switches, although in this work we used a TMAA with single–pole double–throw (SPDT) switches because such architecture provides higher power efficiency [10]. Fig. 1 shows a diagram of the TMAA used in the experiment. It consists of four sections and each section is composed of two oppositely arranged series–fed double–patch antennas. Sections are numbered with $n = 0 \ldots 3$. In each section signals received by oppositelly arranged antennas are delivered to an SPDT microwave switch, which operates alternatively in such a way, that the upper antenna is active for duration τ_n and the lower antenna is active for duration $T_0 - \tau_n$ (the switching is periodical with period T_0). Two received signals have 180° phase difference hence, the output signal $y_n(t)$ has a waveform of a binary phase-keyed signal. Operation of SPDT switches with oppositely arranged antennas can be represented with rectangular bipolar modulating functions $m_n(t)$ with a high value of 1 and a low value of -1. The modulating functions can be expressed as a combination of complex Fourier series coefficients $M_n^{(q)}$ [11]:

978-9-0827-9703-9/19/$31.00 ©2019 IEEE

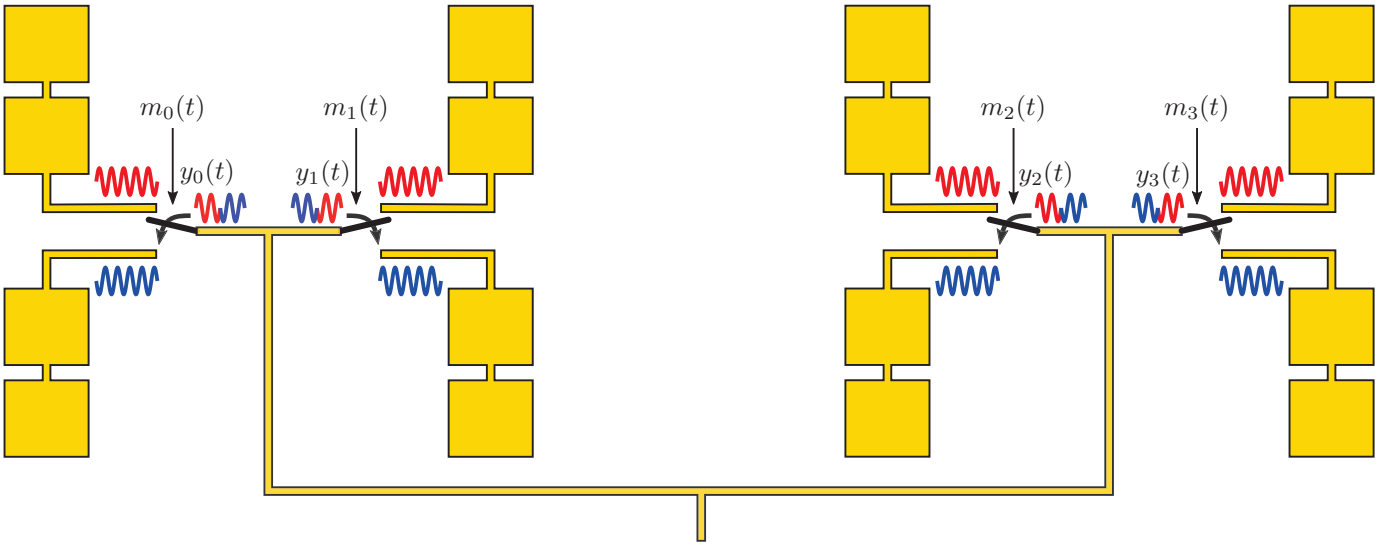

Fig. 1. Diagram of TMAA with SPDT switches

$$m_n(t) = \sum_{k=-\infty}^{\infty} M_n^{(q)} e^{j2\pi f_0 q t} \quad f_0 = \frac{1}{T_0} \tag{1}$$

$$M_n^{(q)} = \frac{1}{T_0} \int_{-T_0/2}^{T_0/2} m_n(t) e^{-j2\pi f_0 q t} dt \tag{2}$$

where: q – number of the frequency component. Hence, spectrum of the signal at the output of TMAA is composed of spectral components (sidebands) located at multiples of the modulation frequency around the center frequency. Example of such spectrum is presented in Fig. 2. Sidebands may be harmfull in some applications, therefore many techniques of suppresion were proposed [12], [13]. On the other hand, they can be usefully utilized for beam-steering [11], wireless communication [14], diversity reception [15], spatial multiplexing [16], and direction of arrival estimation [17]. One of the most usefull properties of the TMAA is the capability of radiation pattern shaping at sideband frequencies, which is known as harmonic beamforming [11]. Fig. 4 shows examples of beam-steered radiation patterns measured at the first negative spectral components ($q = -1$) and the first positive spectral components ($q = +1$).

III. Experimental setup

The experimental setup was comprised of:

1) a software defined radio (SDR) unit,
2) TMAA connected to a single receiving RF chain (Rx),
3) a pair of omnidirectional antennas connected to two transmitting RF chains (Tx1 and Tx2).

The devices are presented in Fig. 5.

Experiment was performed in a non line-of-sight multipath environment inside a small laboratory with many reflecting surfaces. Distance between omnidirectional antennas and the TMAA was 2 m. NI USRP-2944 [18] was used as the SDR

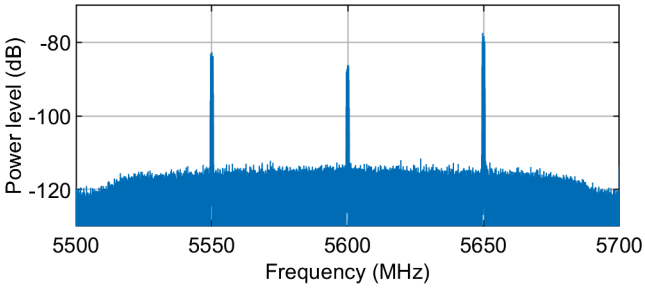

Fig. 2. Spectrum of signal after time modulation

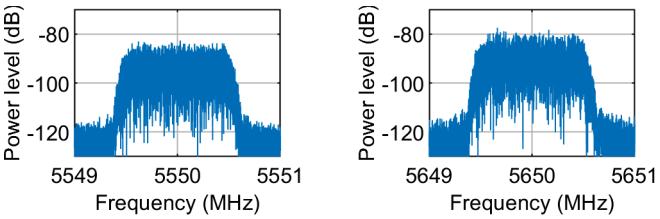

(a) (b)

Fig. 3. Two spectral replicas: (a) $q = -1$; (b) $q = +1$.

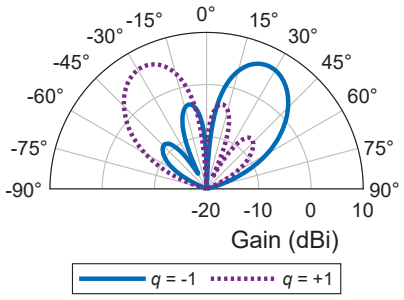

Fig. 4. Radiation patterns of sideband components

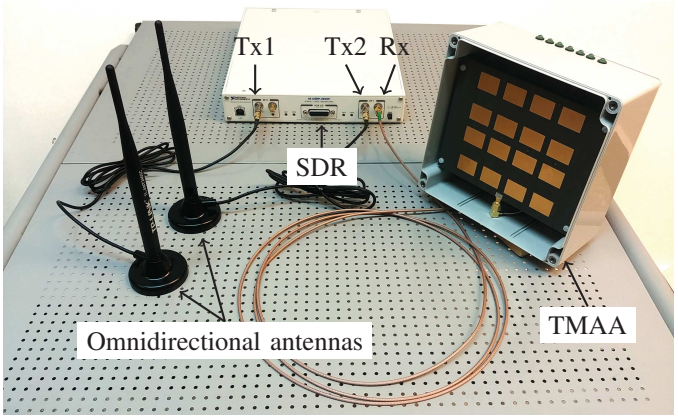

Fig. 5. Experimental setup

unit. Settings of the SDR are gathered in Tab. I. It comprises two full-duplex wideband transceivers, therefore one SDR unit could be used for both the transmitting part and the receiving part. Each transceiver covers frequencies from 10 MHz to 6 GHz with 160 MHz of analog bandwidth. Both transceivers within the SDR unit are coherent and phase-aligned which facilitate development of MIMO applications. Settings of the SDR applied in the experiment are gathered in Tab. II.

A. Transmitting part

A pseudo-random binary sequence (PRBS12) was chosen to form a single data frame to be transmitted over the wireless channel. It was processed in the following way. First, it was alternatively split to form two bit streams. Then, each bit stream was mapped to quadrature phase shift keying (QPSK) modulation scheme to obtain complex baseband samples ($\mathbf{x}_1$ and $\mathbf{x}_2$). Next, samples were filtered with root raised cosine (RRC) filter with roll-off factor $\beta = 0.22$ and upconverted to frequency 5.6 GHz. Finally, filtered and upconverted samples $\hat{\mathbf{x}}_1$ and $\hat{\mathbf{x}}_2$ were transmitted with symbol rate 1 MS/s from Tx1 and Tx2, respectively.

B. Receiving part

The receiving part of the experimental setup was based on the TMAA connected to a single receiving chain (Rx) of the SDR unit. The TMAA used in the experiment have 7 dBi of gain and can be used with wideband signals due to the very high modulation frequency $f_p = 50$ MHz [19]. Spectrum of the signal received by the TMAA and delivered to the receiver is presented in Fig. 2. The signal after time modulation consists of the central component and sideband components located at multiples of 50 MHz around the center frequency. Two useful spectral components at $f^{(-1)} = 5550$ MHz (negative sideband) and $f^{(+1)} = 5650$ MHz (positive sideband), where $f^{(q)}$ denotes the center frequency of the q-th sideband component, are presented in Fig. 3. Radiation patterns measured at these two frequencies were diverse (symmetrical in respect to 0°), i.e. beams were directed toward 30° and −30° for $q = -1$ and $q = +1$, respectively as presented in Fig. 4. Therefore, spectral components consist of replicas of signal received from different angles hence, in conditions of multipath propagation, can be usefully utilized as statistically independent spatial channels.

TABLE I
PARAMETERS OF SDR UNIT [18]

Parameter	Transmitter	Receiver
Number of channels	2	
Frequency range	10 MHz to 6 GHz	
Maximum bandwidth	160 MHz	160 / 84 MHz[a]
Maximum I/Q sample rate	200 MS/s	

[a]Receiver path has 84 MHz of bandwidth from 10 MHz to 500 MHz.

TABLE II
SETTINGS OF EXPERIMENT

Center frequency, $f^{(0)}$	5.6 GHz
Receiver sampling rate	200 MHz
Transmitter symbol rate	1 MS/s
Sample duration, T_s	5 ns
Pulse shaping filter	raised-cosine, $\beta = 0.22$
Modulation scheme	QPSK
MIMO type	2×2, spatial multiplexing

IV. 4D ARRAY SIGNAL PROCESSING FOR MIMO

A. Creation of two MIMO channel output streams

The signal from TMAA was firstly downconverted and then sampled with frequency 200 MHz by the SDR. Then, obtained IQ samples were post-processed in MATLAB. The first step of the post processing was to create two spatial streams from one stream of baseband samples. Each spatial stream was created by demultiplexing, i.e. taking into account only desired sideband (either negative or positive) and filtering out other spectral components. Demultiplexing was accomplished by means of typical signal processing techniques: digital frequency-conversion and low pass filtration. In the experiment the baseband samples obtained from SDR (y_0) were post-processed on a personal computer (PC). Firstly, the original signal was either up or down converted in digital domain by 50 MHz to frequency-shift desired replica to center frequency of the baseband (0 Hz):

$$y_q[n] = y_0[n] e^{-2i\pi q f_0 n T_s} \tag{3}$$

where: q – number of the spectral component (-1 or $+1$), $y_q[n]$ – n-th sample of the q-th stream, f_0 – modulation frequency, T_s – sample duration. Next, the signal was filtered to remove unwanted spectral components. Root raised–cosine filter with roll-off factor $\beta = 0.22$ was used to achieve two effects: remove unwanted components and minimize intersymbol interference. This procedure was done for each $q = -1$ and $q = +1$ to obtain two streams y_{-1} and y_{+1}, which are considered as output streams of a multipath fading channel.

B. Synchronization and decimation

Three types of synchronization were applied: carrier synchronization, symbol synchronization, and frame synchronization.

1) Carrier synchronization: Synthesizers of both transceivers of the SDR are synchronized for the purpose of coherent demodulation. Nevertheless, in our case the carrier recovery was necessary to estimate and compensate frequency difference between the sideband and the receiver's local oscillator. This difference was caused by jitter of the time modulating circuitry, i.e. switches and the control circuit.

A blind FFT-based technique for coarse frequency corrections [20] was applied. The offsets were estimated around -470 Hz and 470 Hz for the first negative and the first positive sideband component, respectively.

2) Symbol synchronization and frame synchronization: The samples were oversampled in the receiver (symbol rate was 1 MS/s and the sampling frequency was 200 MHz) therefore had to be decimated with factor $K = 200$. Signals before and after decimation are presented in Fig. 6. Beginning of the frame was identified by using method of correlation between received samples and known preamble.

C. Channel equalization and symbol detection

Two streams transmitted over a multipath channel are received as:

$$\begin{cases} y_{-1} = h_{-1,1}x_1 + h_{-1,2}x_2 + v_1 \\ y_{+1} = h_{+1,1}x_1 + h_{+1,2}x_2 + v_2 \end{cases} \tag{4}$$

where: y_q – signal received at the q-th sideband component, x_m – symbol transmitted from the m-th antenna, $h_{q,m}$ – channel impulse response between m-th transmitting antenna and q-th sideband component, v_m – noise received at the m-th antenna. Equation (4) can be also expressed in an equivalent matrix notation:

$$\mathbf{y} = \mathbf{H}\mathbf{x} + \mathbf{v}. \tag{5}$$

In our experiment symbols were detected by using the zero forcing (ZF) algorithm:

$$\widetilde{\mathbf{x}} = \mathbf{H}^{\dagger}\mathbf{y}, \tag{6}$$

where $\mathbf{H}^{\dagger} = (\mathbf{H}^H\mathbf{H})^{-1}\mathbf{H}^H$ (in our experiments the channel matrix was square and assumed to be invertible, hence $\mathbf{H}^{\dagger} = \mathbf{H}^{-1}$ [21]). Values of $\mathbf{H}$ were estimated based on a known preamble transmitted over the multipath channel. Samples $\widetilde{\mathbf{x}}_1$ and $\widetilde{\mathbf{x}}_2$ after detection were located in relevant decision regions (Fig. 7), hence all symbols could be successfully demodulated without errors which proves that the TMAA can be used to design a receiver for 2×2 MIMO system with single physical RF chain.

One can notice distortion of samples $\widetilde{\mathbf{x}}_2$ presented in Fig. 7(b). Such effect is caused by fluctuations of the sideband frequency introduced by the jitter of the modulating circuitry. Apparently, the algorithm applied for coarse carrier recovery was not sufficient, therefore additional fine tuning should be implemented. This issue will be addressed in future work.

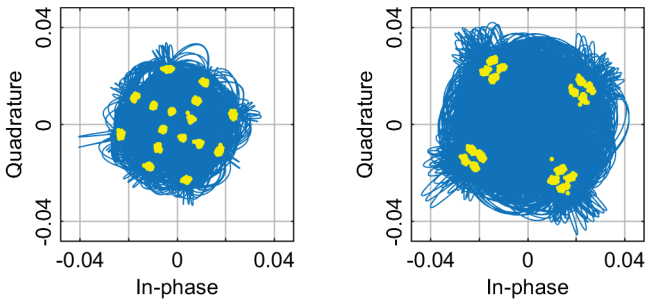

(a) (b)

Fig. 6. IQ samples (a) $q = -1$; (b) $q = +1$

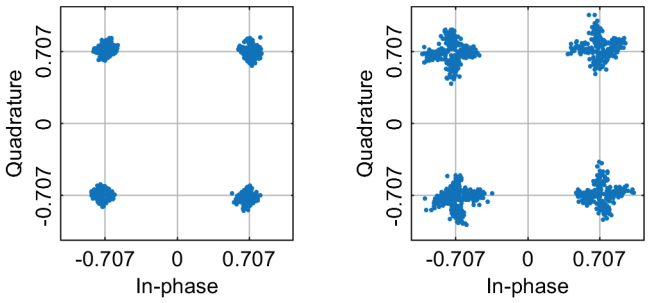

(a) (b)

Fig. 7. IQ symbols after channel equalization (a) $q = -1$; (b) $q = +1$.

V. Conclusion

The problem of multiple RF chains in MIMO system has been solved with 4D array processing. Single wideband receiver with TMAA was used instead of two receivers connected to separate antennas. Therefore cost and power consumption of the 2×2 MIMO receiver was substantially decreased. Two spatial channels were obtained by demultiplexing spectral components generated by the TMAA. Statistical independence between two streams was achieved by means of the beam-steering, i.e. two beams were directed toward -30° and 30°, thus multipath signals were received from distinct directions. Hence, the TMAA with beam-steering functionality can be used to exploit properties of the multipath propagation channel and create two spatial streams with low correlation to facilitate MIMO transmission. Conclusions of this work can be extended further to the massive MIMO systems, where benefits from reducing number of RF chains can be even more encouraging.

References

[1] G. Foschini and M. Gans, "On limits of wireless communications in a fading environment when using multiple antennas," *Wireless Personal Communications*, vol. 6, no. 3, pp. 311–335, Mar. 1998.

[2] S. Sanayei and A. Nosratinia, "Antenna selection in MIMO systems," *IEEE Commun. Mag.*, vol. 42, no. 10, pp. 68–73, Oct. 2004.

[3] A. K. Sah and A. K. Chaturvedi, "Quasi-orthogonal combining for reducing RF chains in massive MIMO systems," *IEEE Wireless Commun. Lett.*, vol. 6, no. 1, pp. 126–129, Feb 2017.

[4] A. Alkhateeb, Y.-H. Nam, J. Zhang, and R. W. Heath, "Massive MIMO combining with switches," *IEEE Wireless Commun. Lett.*, vol. 5, no. 3, pp. 232–235, Jun. 2016.

[5] M. A. Jensen and J. W. Wallace, "A review of antennas and propagation for MIMO wireless communications," *IEEE Trans. Antennas Propag.*, vol. 52, no. 11, pp. 2810–2824, Nov. 2004.

[6] S. Saunders and A. Aragón-Zavala, *Antennas and Propagation for Wireless Communication Systems*, 2nd ed. John Wiley & Sons, 2007.

[7] R. Maneiro-Catoira, J. Brégains, J. A. García-Naya, and L. Castedo, "Time modulated arrays: from their origin to their utilization in wireless communication systems," *Sensors*, vol. 17, no. 3, p. 590, Mar. 2017.

[8] J. P. González-Coma, R. Maneiro-Catoira, and L. Castedo, "Hybrid precoding with time-modulated arrays for mmwave MIMO systems," *IEEE Access*, vol. 6, pp. 59 422–59 437, 2018.

[9] G. Bogdan, K. Godziszewski, Y. Yashchyshyn, and S. Kozłowski, "Single RF chain MIMO receiver using beam-steering time modulated antenna array," in *13th Eur. Conf. Antennas Propag. (EuCAP)*, Kraków, Poland, Apr. 2019.

[10] G. Bogdan, Y. Yashchyshyn, and M. Jarzynka, "Time-modulated antenna array with lossless switching network," *IEEE Antennas Wireless Propag. Lett.*, vol. 15, pp. 1827–1830, 2016.

[11] L. Poli, P. Rocca, G. Oliveri, and A. Massa, "Harmonic beamforming in time-modulated linear arrays," *IEEE Trans. Antennas Propag.*, vol. 59, no. 7, pp. 2538–2545, Jul. 2011.

[12] S. Yang, Y. B. Gan, and A. Qing, "Sideband suppression in time-modulated linear arrays by the differential evolution algorithm," *IEEE Antennas Wireless Propag. Lett.*, vol. 1, pp. 173–175, 2002.

[13] L. Poli, P. Rocca, L. Manica, and A. Massa, "Time modulated planar arrays - analysis and optimisation of the sideband radiations," *IET Microw. Antennas Propag.*, vol. 4, no. 9, pp. 1165–1171, Sep. 2010.

[14] R. Maneiro-Catoira, J. C. Brégains, J. A. García-Naya, and L. Castedo, "On the feasibility of time-modulated arrays for digital linear modulations: A theoretical analysis," *IEEE Trans. Antennas Propag.*, vol. 62, no. 12, pp. 6114–6122, Dec. 2014.

[15] R. Maneiro-Catoira, J. C. Brégains, J. A. García-Naya, L. Castedo, P. Rocca, and L. Poli, "Performance analysis of time-modulated arrays for the angle diversity reception of digital linear modulated signals," *IEEE J. Sel. Topics Signal Process.*, vol. 11, no. 2, pp. 247–258, Mar. 2017.

[16] P. Rocca, Q. Zhu, E. Bekele, S. Yang, and A. Massa, "4-D arrays as enabling technology for cognitive radio systems," *IEEE Trans. Antennas Propag.*, vol. 62, no. 3, pp. 1102–1116, Nov. 2014.

[17] G. Li, S. Yang, and Z. Nie, "Direction of arrival estimation in time modulated linear arrays with unidirectional phase center motion," *IEEE Trans. Antennas Propag.*, vol. 58, no. 4, pp. 1105–1111, Apr. 2010.

[18] *Specifications USRP-2944 Software Defined Radio Reconfigurable Device*, National Instruments, 2017. [Online]. Available: http://www.ni.com/pdf/manuals/375724b.pdf

[19] G. Bogdan, K. Godziszewski, Y. Yashchyshyn, C. H. Kim, and S. Hyun, "Time modulated antenna array for real-time adaptive beamforming in wideband wireless systems–part 1: Design and characterization," *IEEE Trans. Antennas Propag.*, vol. 67, 2019.

[20] Y. Wang, K. Shi, and E. Serpedin, "Non-data-aided feedforward carrier frequency offset estimators for QAM constellations: A nonlinear least-squares approach," *EURASIP J. Adv. Signal Process.*, vol. 2004, no. 13, pp. 1993–2001, Oct. 2004.

[21] S. Yang and L. Hanzo, "Fifty years of MIMO detection: The road to large-scale MIMOs," *IEEE Commun. Surveys Tuts.*, vol. 17, no. 4, pp. 1941–1988, Oct.-Dec. 2015.